

# Comparison of Electromagnetic Solvers for the Analysis of LTCC Components

Luca Pierantoni\*, Marco Farina\*, Tullio Rozzi\*, Fabio Coccetti\*\*\*, Peter Russer\*\*,  
Nathan Bushyager\*\*\*, Manos Tentzeris\*\*\*

Dipartimento di Elettronica, University of Ancona – Italian National Institute for Physics of Matter, Italy  
Technische Universität München, Lehrstuhl für Hochfrequenztechnik, Munich, Germany\*\*  
School of ECE, Georgia Institute of Technology, Atlanta, GA 30332-250, USA\*\*\*

**Abstract** In this contribution we present an accurate modeling of complex vertically integrated structures based on the new LTCC multilayer technology. The EM analysis is performed by means of different electromagnetic full-wave solvers in the time- and frequency-domains. We analyze a stacked patch antenna and a spiral inductor. The calculated S-parameters and Q-factors are compared to measured data showing good agreement.

## I. INTRODUCTION

Emerging applications in RF/microwave/millimeter wave regimes require minimization, portability, cost and performance as key driving forces in this evolution. Multiband applications are also becoming extremely important within passive development to realize multiple frequency bands and multiple standards for various wireless and WLAN (802.11x) applications. Investigations on System on Package have become a primary focus due to the real estate efficiency, cost-saving and performance improvement potentially involved in this integrated functionality. Design flexibility and optimized integration of embedded functions, such as antennas, can be easily achieved with multilayer substrate technologies such as multilayer low-temperature co-fired ceramic (LTCC) and multilayer organic (MLO) materials, [1,2,3]. One of the major challenges in the development of the multilayer modules is the accurate modeling of embedded resonant structures such as antennas and passives (e.g. inductors). Typically, these geometries exhibit several fine geometrical details, finite thickness dielectric layers, losses, thick metals of arbitrary shape and very large "aspect-ratios".

In this paper we evaluate the simulation performance of four full-wave 3D-solvers based on different methods in the time- and frequency-domains, namely i) Finite Difference in Time-Domain (FDTD); ii) Transmission Line Matrix (TLM); iii) Transmission Line Matrix - Integral Equation (TLM-IE); iv) Generalized Transverse Resonance Diffraction (GTRD).

FDTD and TLM are time-domain space discretizing methods that allow for the numerical full-wave modeling of structures with nearly arbitrary geometry [4,5]. Their disadvantages appear when dealing with large homogeneous (i.e. bulk, free-space) regions which augment considerably the 3D-spatial domain of computation, thus increasing the number and the size of the elementary cells. To some extent, this problem can be alleviated by using perfectly-matched layers (PML) as numerical absorbers. The hybrid TLM-IE method combines the advantages of the TLM technique with the computational superiority of the IE method for wide homogeneous regions, [6]. A minor drawback is the need of the storage of the time-evolution of the tangential field in order to guarantee an efficient coupling of the TLM and the Green's function-based Integral Equation. In [7] a 3D GTRD formulation for boxed multilayer structures was presented that exploited the Green's function of a loaded box and was shown to be especially suited for MMIC and MEMS analysis. Four full-wave numerical solvers were developed based to the aforementioned techniques including computer tools for pre and post processing and computer visualization [5]: three of them are in time-domain while only GTRD is in frequency-domain. By using the above methods, we have calculated S-parameters, radiation pattern and Q-factor and compared them to measured results, with good agreement.

## II. THEORY

The finite-difference time-domain (FDTD) method is a very popular full-wave technique that discretizes the curl Maxwell equations and calculates the time-evolution of the electromagnetic field. It is very versatile and has been shown to give very accurate simulation results for a variety of structures. However, the smallest feature of the modeled device limits the size of structures that can be simulated in FDTD. When elements with very fine details

are combined into geometries containing large connecting structures, the resulting grid can grow beyond the capability of most computers. Several techniques can be applied to an FDTD implementation to reduce the grid size while maintaining required accuracy. Three of the most common ways to increase computational efficiency are the code parallelization, the addition of a variable grid and the use of DSP-based spectral estimators.

In the TLM method the evolution of the discretized electromagnetic field is modeled by wave voltage and current pulses propagating on a mesh of transmission lines and scattered at the mesh nodes [3,4].

In the TLM-IE method the 3D space is segmented into different sub-regions, where the best suited method, be it TLM or IE, is applied. Inside the TLM-regions, the electromagnetic field is modeled by the TLM method. In IE-regions the EM field is calculated analytically by means of the appropriate Green's function. The continuity of the field is applied at the interfaces between regions, providing appropriate integral equations for the tangential field which represents the exact boundary condition for the TLM algorithm [6].

In the GTRD approach the Green's function of a horizontally uniform multilayer dielectric stack is calculated [7] and links fields within the stack to arbitrary current source distributions through

$$\mathbf{E}(\mathbf{r}) = - \iiint_V d\mathbf{r}' \mathbf{Z}(\mathbf{r}, \mathbf{r}') \cdot \mathbf{J}(\mathbf{r}') \quad (1)$$

Lossy conductors and non-uniform dielectrics are described by specifying the nature and the location of the volume sources  $\mathbf{J}$ . In particular Ohm's law is imposed to hold *in* conductors, and displacement currents are defined within the dielectric discontinuities (dielectric bricks). The two conditions may be expressed in just one equation, provided that the standard complex permittivity definition is used:

$$j\omega\epsilon_0(\tilde{\epsilon}(\mathbf{r}) - \tilde{\epsilon}'(\mathbf{r}))\mathbf{E}(\mathbf{r}) = \mathbf{J}(\mathbf{r}) \quad (2)$$

where primed permittivity indicates the embedding medium ( $\epsilon, \sigma$ ) whose boundary conditions are already included when writing condition (1). By substituting (2) in (1) an eigenvalue integral equation would be obtained and can be turned into a deterministic one by defining standard delta-gap field excitation. This integral equation can be solved by using Galerkin's method, obtaining the current distribution  $\mathbf{J}$ .

For a given set of ports, if one port is excited while the other ones are shorted to the ground (enclosure box),  $\mathbf{J}$  directly provides the short circuit admittance matrix  $\mathbf{Y}$ , to

be suitably converted in  $\mathbf{S}$ . The source discontinuity gets removed by appropriate de-embedding.

### III. RESULTS

#### LTCC-Antenna

Fig.1 shows the analyzed microstrip-fed stacked-patch antenna on LTCC multilayer substrate [1] for LMDS applications. The dimensions of the patches are 2.032x2.032 mm; metal thickness, material parameters and losses are shown in the sketch. We note a strong "aspect ratio" of about 700. In Fig.2 we report the comparison among the Return-Loss (vs. frequency) calculated by the different methods. Results indicate that all methods are in good agreements. Resonant frequencies (in GHz) are: FDTD:  $f=28$ ; TLM:  $f=28.1$ ; TLM-IE:  $f=28.3$ ; GTRD:  $f=28.7$ . The slight frequency shift of GTRD is currently under investigation. Table I indicates the resources required by different approaches. It is remarkable to observe that by using the TLM-IE method both the bulk LTCC-region and the free-space regions are modeled by means of the appropriate Green's function, thus drastically reducing the 3D spatial domain of computation for the TLM algorithm [6].

GTRD shows a fairly high computational cost. This is related to our intent of including the cavity around the patch by means of 3D conductors instead of exploiting the enclosure box. This way GTRD capability in handling 3D objects is fully exploited, while it is clear that GTRD obtains best performance where planar nature dominates and the cross-sectional aspect ratio is the most critical one. In fact 3D thick objects require a sufficient subsectioning along the thickness direction when solving the integral equation, while on the other hand, any complex substrate is directly modeled by the Green's function, and may only affect marginally the computational load.

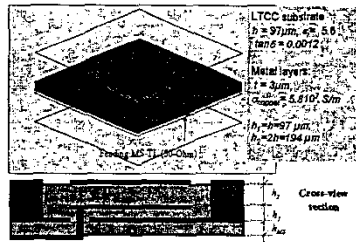


Fig.1 The LTCC microstrip-fed stacked-patch antenna

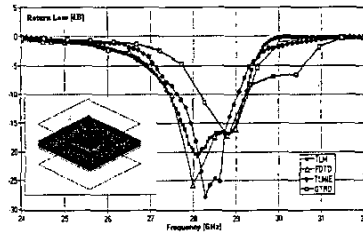


Fig. 2. Comparison of the results for the LTCC-antenna of Fig. 1: Return Loss (dB) versus frequency [GHz].

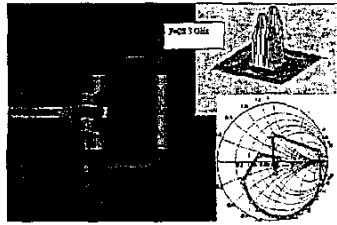


Fig. 3. Patch antenna. Current distribution (left and right-up side) at  $f=28.3$  GHz. Smith-Chart (right-down side).

method	mesh/resolution	CPU-time	Mb-Ram
FDTD	210x72x206	~9.5 Hrs Athlon MP 1800	170
TLM	240x138x62	~10 Hrs (HP C-360)	147
TLM-IE	160x120x30	~2 Hrs PC-Pent.II 500 MHz	130
GTRD	82x82 (modes)	~10 Hrs PC-Pent.II 500 MHz	350

Tab.1. Comparison of computational data for the antenna.

In Fig.3 we report the current density distribution (left and right-up side) at  $f=28.3$  GHz. Smith chart is also inserted in right-down side. These figures are produced by using the post-processing tools of the GTRD solver [7]. It has to be stressed that LTCC-embedded antennas offer a unique design opportunity. Modifying the thickness and the number of LTCC layers can tune appropriately the bandwidth, the resonant frequency, the radiation pattern and the integrability with the rest of the vertically integrated structures. Thus, it is imperative to have a good multifrequency representation of all these figures of merit.

#### LTCC-Spiral Inductor

The second analyzed structure was chosen to be the spiral-inductor depicted in Fig.4, that has been built-up on a LTCC-substrate for WLAN 802.11a applications. The simulation of this type of structures is very challenging due to its large aspect ratio and its highly resonant character that, when using time-domain techniques, requires the modeling over a large period. Thus, this topology is very sensitive even to very small variations of mesh size and material parameters. In Fig.5 we compare the Q-factor (dB) calculated by the different methods. It is remarkable to note that all the solvers produce accurate results: TLM, TLM-IE and experimental data change the nature of the reactance (from inductance to capacitance) around  $f=8.4$  GHz, whereas GTRD at  $f=8.0$  GHz and FDTD does it at  $f=7.4$  GHz for 200,000 steps and the use of a DSP predictor. Moreover Q-factor in FDTD shows a stronger gradient around this frequency. Finally, in Fig.6 we report the simulated current density distribution at  $f=3.8$  GHz and  $f=8.5$  GHz. The figures are produced by the GTRD solver. Having an accurate picture of this distribution helps in the optimization of this inductor structure, since it allows for the identification and modification of areas of high parasitic coupling. Also, the 3D field variation will help in the effective choice of the thickness of the LTCC layers, based on resonant frequency, bandwidth and parasitics.

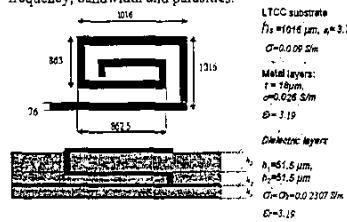


Fig.4. LTCC spiral inductor.

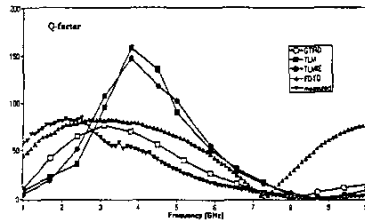


Fig. 5. Comparison of the calculated Q-factor (dB) for the inductor of Fig 4

#### IV. CONCLUSIONS

The performances of the four full-wave approaches, FDTD, TLM, TLM-IE and GTRD, have been compared for the case of complex multilayer LTCC structures. All of them show good agreement in the evaluation of S-parameters and Q-factor, something that would enable the effective design and optimization of future LTCC vertically integrated transceivers.

#### ACKNOWLEDGEMENTS

The authors wish to acknowledge the support of the Georgia Tech NSF Packaging Research Center, the Yamacraw Research Center of the State of Georgia, the Deutsche Forschungsgemeinschaft and the NSF CAREER Grant 9984761.

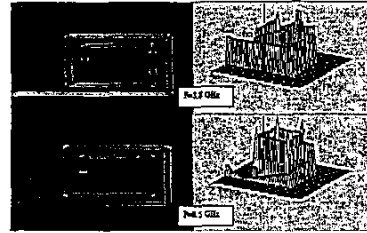


Fig.6.Spiral inductor. Distribution of the current density at  $f=3.8$  GHz (up) and  $f=8.5$  GHz (down).

#### REFERENCES

- [1] R.L.Li, K.Lim, M.Maeng, E.Tsai, G.Dejean, M.Tentzeris and J.Laskar, "Design of Compact Stacked-Patch Antennas on LTCC Technology for Wireless Communication Applications" *Proc. 2002 IEEE AP-S Symposium*, San Antonio, TX, June 2002, pp.11.500-503.
- [2] N.Bushyager, M.Davis, E.Dalton, J.Laskar and M.Tentzeris, "Q-Factor Prediction and Optimization of Multilayer Inductors for RF Packaging Microsystems Using Time-Domain Techniques", *Proc. of the 2002 IEEE Electronic Components and Technology Conference*, San Diego, CA, May 2002, pp.1718-1721.
- [3] K.Lim, S.Pinel, M.Davis, A.Suzono, C.-H.Lee, D.Heo, A.Obatayinbo, J.Laskar, E.M.Tentzeris, R.Tummla, "RF-System-On-Package (SOP) for Wireless Communications", *IEEE Microwave Magazine*, Vol.3, No.1, pp.88-99, March 2002.
- [4] A.Taflov and S.Hagness, *Computational Electrodynamics, the finite difference time domain approach*, 2nd ed., Boston, Artech House, 2000.
- [5] P. Russer, "The transmission line matrix method", *Applied Computational Electromagnetics*, NATO ASI Series.
- [6] L. Pierantoni, S. Lindenmeier and P. Russer, "Efficient analysis and modeling of the radiation of microstrip lines and patch antennas by the TLM-integral equation (TLM-IE) method", *International Journal of Numerical Modelling: Electronic Networks, Devices and Fields*, vol.12, nr.4, July-Aug.1999, pp.329-340.
- [7] M. Farina, T. Rozzi, "A 3-D integral equation-based approach to the analysis of real-life MMICs: application to microelectromechanical systems", *IEEE Trans. Microwave Theory and Tech.*, vol. 49, no. 12 December 2001, pp. 2235-2240.